

# General Relativistic effect on the energy deposition rate for neutrino pair annihilation above the equatorial plane along the symmetry axis near a rotating neutron star

Abhijit Bhattacharyya<sup>c</sup>, Sanjay K. Ghosh<sup>a,b\*</sup>, Ritam Mallick<sup>a,b†</sup>, , and Sibaji Raha<sup>a,b</sup>

<sup>a</sup>*Department of Physics; Bose Institute; 93/1,*

*A.P.C Road; Kolkata - 700009; INDIA*

<sup>b</sup>*Centre for Astroparticle Physics and Space Science; Bose Institute; 93/1,*

*A.P.C Road; Kolkata - 700009; INDIA and*

<sup>c</sup>*Department of Physics; University of Calcutta; 92,*

*A.P.C Road; Kolkata - 700009; INDIA*

(Dated: May 30, 2019)

## Abstract

The estimate of the energy deposition rate (EDR) for neutrino pair annihilation has been carried out. The EDR for the neutrinos coming from the equatorial plane of a rotating neutron star is calculated along the rotation axis using the Cook-Shapiro-Teukolsky (CST) metric. The neutrino trajectories and hence the neutrino emitted from the disk is affected by the redshift due to disk rotation and gravitation. The EDR is very sensitive to the value of the temperature and its variation along the disk. The rotation of the star has a negative effect on the EDR, it decreases with increase in rotational velocity.

PACS numbers: 97.60.Jd, 26.60.+c

---

\* Email : sanjay@bosemain.boseinst.ac.in

† Email : ritam@bosemain.boseinst.ac.in

## I. INTRODUCTION

Gamma Ray Bursts (GRB), first discovered in the late 1960s by US military satellites [1], and its possible connection with neutrino production in compact stars is a field of high current interest. The central engine of GRBs is still shrouded in a mist, although several models has been proposed. GRBs are separated in two classes; long duration bursts (long GRB) which lasts from 2 second to several minutes, with average duration of 30 seconds and short duration bursts (short GRB), with burst duration from few milliseconds to 2 second, average being 0.3 seconds. Of late, the detection of afterglows in short GRBs and also precise localization of different short GRBs have provided new inputs for the study of these phenomena. The light curves [2] and polarization [3] of gamma ray burst afterglows indicate anisotropic central engines. These observations have been considered as evidence that GRBs are highly beamed.

Neutron stars are objects formed in the aftermath of supernova. The central density of these stars can be as high as 10 times that of normal nuclear matter. At such high density, any small perturbation, *e.g.* spin down of the star, may trigger a phase transition from nuclear to quark matter system. As a result, the neutron star may convert to a quark star or a hybrid star with a quark core [4, 5, 6]. It has been shown [7] that such a phase transition [8] produces a large amount of high energy neutrinos. These neutrinos (and antineutrinos) could annihilate and give rise to electron-positron pairs through the reaction  $\nu\bar{\nu} \rightarrow e^+e^-$ . These  $e^+e^-$  pairs may further give rise to gamma rays which may provide a possible explanation of the observed GRB. Furthermore, the rotating neutron stars have been shown [9] to produce the observed beaming effect. At present, it is necessary to have a better understanding of the energy deposition in the neutrino annihilation to  $e^+e^-$  process in the realistic neutron star environment.

Motivated by the delayed explosion of Type II supernovae, the EDR due to the reaction  $\nu\bar{\nu} \rightarrow e^+e^-$  in the vicinity of a neutron star have been calculated [10, 11] based on Newtonian gravity, *i.e.*  $(2GM/c^2R) \ll 1$ . Goodman *et al.* [11] pointed out that the neutrino pair annihilation rate can be seriously altered by the gravitational effects. The effect of gravity was incorporated in refs. [12, 13], but only for a static star. Slow rotation on this calculation was introduced by Prasanna and Goswami [14]. GR effect on energy deposition rate for neutrino pair annihilation near a black hole was studied in ref. [15, 16] to explore the

possible engine for GRBs. Here the most probable candidate for the central engine was the accretion disk around a black hole. A detailed hydrodynamic simulation of the process was studied by Birkel *et al.* [17].

The relativistic effect consists of three factors: the gravitational redshift, the bending of the neutrino trajectories and redshift due to rotation. The EDR is enhanced by the effect of neutrino bending, however the redshift due to disc rotation and gravitation reduces the EDR. Thus these effects further complicate the estimation of EDR. In order to discuss quantitatively the central engine of GRBs, we need a comprehensive study of the formation, evolution, temperature dependence, geometry of the star, the mechanism of energy deposition etc., most of which are affected by the rotational and GR effect.

In an earlier paper [18] we have shown that the path of neutrino is important for the study of EDR near a massive object. We have done a complete GR calculation of the neutrino path for the most general metric describing a rotating star, and obtained its geodesic equation along the equatorial and polar plane. The minimum photosphere radius (MPR) has been calculated for various stars along these two planes. Our aim in this work is to study semianalytically the relativistic effect on the EDR above the equatorial plane for a star rotating along the polar axis. We calculate the EDR along the rotation axis for the neutrinos coming from the equatorial plane of the star.

Our paper is arranged as follows. In the next section we fix our EOS and describe the geometry of the star. In section III we formulate the algorithm of the EDR calculation above the equatorial plane along the rotation axis. Next we present our results and finally we discuss the results and summarize our work.

## II. STAR STRUCTURE

The structure of the star is described by the CST metric given by [19]

$$ds^2 = -e^{\gamma+\rho} dt^2 + e^{2\alpha}(dr^2 + r^2 d\theta^2) + e^{\gamma-\rho} r^2 \sin^2\theta (d\phi - \omega dt)^2. \quad (1)$$

The four gravitational potentials, namely  $\alpha, \gamma, \rho$  and  $\omega$  are functions of  $\theta$  and  $r$  only. All the potentials have been solved for both static as well as rotating stars using the 'rns' code [20, 21, 22]. For a rotating star, all the potentials become functions of both  $r$  and  $\theta$ .

Tabulated equations of state (EOS) are needed to compute the code numerically. In

this paper we have used hadronic EOS evaluated using the nonlinear Walecka model [23]. The Lagrangian in the model includes nucleons (neutrons and protons), electrons, isoscalar scalar, isoscalar vector and isovector vector mesons denoted by  $\psi_i$ ,  $\psi_e$ ,  $\sigma$ ,  $\omega^\mu$  and  $\rho^{a,\mu}$ , respectively. The Lagrangian also includes cubic and quartic self interaction terms of the  $\sigma$  field. The parameters of the nonlinear Walecka model are meson-baryon coupling constants, meson masses and the coefficient of the cubic and quartic self interaction of the  $\sigma$  mesons. The meson fields interact with the baryons through linear coupling. The  $\omega$  and  $\rho$  meson masses have been chosen to be their physical masses. The rest of the parameters, namely, nucleon-meson coupling constants and the coefficients of cubic and quartic terms of the  $\sigma$  meson self interaction are determined by fitting the nuclear matter saturation properties, namely, the binding energy/nucleon (-16 MeV), baryon density ( $\rho_0=0.17 \text{ fm}^{-3}$ ), symmetry energy coefficient (32.5 MeV), Landau mass ( $0.83 m_n$ ) and nuclear matter incompressibility (300 MeV).

Using this tabulated EOS and a fixed central density, the **rns** code is solved to obtain all the gravitational potentials as a function of  $r$  and  $\theta$ , which thereby defines the shape, mass, rotational velocity and other parameters of the star. The shape of a fast rotating neutron star becomes oblate spheroid [19]. The star gets compressed along the z-axis, on the other hand along x and y-axes it bulges by equal amounts, the polar radius thus being smaller than equatorial radius.

### III. GR CALCULATION

In this section we study the GR effect on the neutrino pair annihilation rate. The coordinate system is oriented in such a way that the equatorial plane lies along  $\theta = \frac{\pi}{2}$  and the polar plane along  $\theta = 0$ . We treat the equatorial plane as a disk from which the neutrinos are coming out and the EDR is calculated along the different radial points on the rotation axis. Here we are interested in the EDR via neutrino pair annihilation near the rotation axis,  $\theta = 0$  [15, 16]. It has been shown earlier [15] that in the absence of gravitation the  $\theta$  dependence of the EDR is weak for small values of  $\theta$ . Although the  $\theta$  dependence of the gravitational effect may not necessarily be small, here we calculate the EDR at  $\theta = 0$  and assume it to be approximately same for small values of  $\theta$ .

The energy deposited per unit volume per unit time is given as [10, 11]

$$\dot{q}(r, \theta) = \int \int f_\nu(p_\nu, r) f_{\bar{\nu}}(p_{\bar{\nu}}, r) (\sigma |v_\nu - v_{\bar{\nu}}| \epsilon_\nu \epsilon_{\bar{\nu}}) \frac{\epsilon_\nu + \epsilon_{\bar{\nu}}}{\epsilon_\nu \epsilon_{\bar{\nu}}} d^3 p_\nu d^3 p_{\bar{\nu}}, \quad (2)$$

where  $f_\nu$  ( $f_{\bar{\nu}}$ ) is the number density of neutrino (antineutrino),  $v_\nu$  is the neutrino velocity, and  $\sigma$  is the rest frame cross section for the process  $\nu\bar{\nu} \rightarrow e^+e^-$ . The Lorentz invariant term is given by

$$(\sigma |V_\nu - V_{\bar{\nu}}| \epsilon_\nu \epsilon_{\bar{\nu}}) = \frac{DG_F^2}{3\pi} (\epsilon_\nu \epsilon_{\bar{\nu}} - p_\nu \cdot p_{\bar{\nu}})^2 \quad (3)$$

with

$$G_F^2 = 5.29 \times 10^{-44} \text{cm}^2 \text{MeV}^{-2}; \quad (4)$$

$$D = 1 \pm 4 \sin^2 \theta_w + 8 \sin^4 \theta_w. \quad (5)$$

$\sin \theta_w = 0.23$ . (+) sign is for electron neutrino-antineutrino pair and (-) sign for other pairs.

As the geometry of the equatorial plane is circular, we can decouple the energy and angular dependence. Thus the rate of energy deposition is

$$\dot{q}(r) = \frac{DG_F^2}{3\pi} F(r) \int \int f_\nu f_{\bar{\nu}} (\epsilon_\nu + \epsilon_{\bar{\nu}}) \epsilon_\nu^3 \epsilon_{\bar{\nu}}^3 d\epsilon_\nu d\epsilon_{\bar{\nu}} \quad (6)$$

where,  $F(r)$ , the angular integral, is given by [16]

$$F(r) = \frac{2\pi^2}{T_{eff}^9} \left( \frac{e^{\gamma+\rho}}{e^{\gamma+\rho} - r^2 \omega^2 \sin^2 \theta e^{\gamma-\rho}} \right)^4 \left( 2 \int_{\theta_m}^{\theta_M} d\theta_\nu T_0^5 \sin \theta_\nu x \int_{\theta_m}^{\theta_M} d\theta_{\bar{\nu}} T_0^4 \sin \theta_{\bar{\nu}} \right. \\ \left. + \int_{\theta_m}^{\theta_M} d\theta_\nu T_0^5 \sin^3 \theta_\nu x \int_{\theta_m}^{\theta_M} d\theta_{\bar{\nu}} T_0^4 \sin^3 \theta_{\bar{\nu}} + 2 \int_{\theta_m}^{\theta_M} d\theta_\nu T_0^5 \cos^2 \theta_\nu \sin \theta_\nu x \int_{\theta_m}^{\theta_M} d\theta_{\bar{\nu}} T_0^4 \cos^2 \theta_{\bar{\nu}} \sin \theta_{\bar{\nu}} \right. \\ \left. - 4 \int_{\theta_m}^{\theta_M} d\theta_\nu T_0^5 \cos \theta_\nu \sin \theta_\nu x \int_{\theta_m}^{\theta_M} d\theta_{\bar{\nu}} T_0^4 \cos \theta_{\bar{\nu}} \sin \theta_{\bar{\nu}} \right). \quad (7)$$

We calculate the energy integral numerically, integrating it from 0 to  $\infty$ . Both the angular and energy integral has temporal component which are affected by the GR and rotational effect.  $T_{eff}$  is the effective temperature of the disc that is observed in the comoving frame. The value of  $T_0$  is the temperature of the disc that is observed at infinity. In the locally nonrotating frame a neutrino moves normally to the direction of the disk motion. In that case, the temperature suffers redshift both due to disk rotation and gravitation. Therefore the two temperature  $T_0$  and  $T_{eff}$  are related [16], as

$$T_0 = \frac{T_{eff}}{\Gamma} \sqrt{g_{tt} - \frac{g_{t\phi}^2}{g_{\phi\phi}}}. \quad (8)$$

$g_{tt}$ ,  $g_{t\phi}$  and  $g_{\phi\phi}$  are calculated from the metric.  $\Gamma$  is the Lorentz factor defined as  $\Gamma = \frac{1}{\sqrt{1-v^2}}$  with  $v$  being  $v = (\Delta - \omega)r\sin\theta e^{-\rho}$ ,  $\Delta$  the rotational velocity of the star.

In an earlier paper [18] a detailed GR calculation of the neutrino path has been done. For the present coordinate system, the 4- momentum [16] is given by the equation,

$$g_{\mu\nu}p^\mu p^\nu + \mu_m^2 = 0, \quad (9)$$

where  $\mu_m$  is the rest mass of the particle and  $p^\mu = \frac{dx^\mu}{d\lambda}$ ,  $\lambda$  being the affine parameter. After a bit of algebra the final geodesic equation can be written as,

$$e^{2\alpha} \left[ \frac{A(r, \theta)}{A(r, \theta) + \omega} \right]^2 \frac{e^{(\gamma-\rho)r^2 \sin^2 \theta}}{e^{2\alpha}} \tan^2 \theta_r \left[ \omega(1 - \omega b) + \frac{e^{2\rho b}}{r^2 \sin^2 \theta} \right]^2 - e^{(\gamma+\rho)} (1 - \omega b)^2 + \frac{b^2}{r^2 \sin^2 \theta} e^{(\gamma+3\rho)} = 0. \quad (10)$$

This equation can be solved using the potentials obtained from **rns** code to obtain a minimum radius  $r = R_{MPR}$ , the minimum photosphere radius, below which a massless particle (neutrino) emitted tangentially to the stellar surface ( $\theta_R = 0$ ) would be gravitationally bound. This is also the minimum radius from which the neutrinos can come out from the disk.

From an angle  $\theta_\nu$  at a point  $(r, 0)$ , we can trace back a trajectory of the neutrino to its emission point on the disc. Thus the temperature  $T_0$  depends on  $\theta_\nu$ , and therefore  $T_{eff}$  appears in the integration of  $\theta_\nu$  in the angular integral. The neutrinos are coming out of the disk and depositing their energy along the rotation (symmetry) axis of the disk. The minimum radius from which the neutrinos can come out is given by MPR. The outermost point from which the neutrinos comes out is from the surface of the disc (*i. e.* the surface of the star along the equatorial plane). Figure 1. shows the layout of our problem, where neutrinos coming out from the disk and are depositing their energy along the rotation axis. The angle from which the neutrinos are coming can be calculated from the figure. The angle  $\theta_m$  is the angle subtended by the MPR on the rotation axis, which is given by

$$\theta_m = \tan^{-1} \frac{R_{MPR}}{r}. \quad (11)$$

where  $R_{MPR}$  is the MPR on the disc. Similarly  $\theta_M$  is the angle subtended by the surface of the star on the rotation axis

$$\theta_M = \tan^{-1} \frac{R_{Sur}}{r}. \quad (12)$$

where  $R_{Sur}$  is the radius of the outer surface of the disc *i. e.* equatorial radius of the star.

The EDR is now calculated by integrating  $\dot{q}$  over the proper volume. We calculate the amount of energy deposited over  $r$  and within  $\theta$  in the close vicinity of the rotation axis [15]. The point on the rotation axis from where we start our calculation is  $r = R_{MPR}$ . In this problem we are considering only the thermal neutrinos and our lower limit of integration is the MPR. Beyond the MPR the density of the star is not as high as that of the central region. Beyond the MPR the thermal neutrinos are transparent to the star and therefore the rate of deposition energy reabsorbed is not so large and we ignore it.

#### IV. RESULTS

We choose the central density of the star to be  $1 \times 10^{15} gm/cm^3$ , for which the Keplerian velocity is  $0.61 \times 10^4 s^{-1}$ . For comparison we have also done the calculation for a slow star ( $0.4 \times 10^4 s^{-1}$ ). For the keplerian star the equatorial radius is  $16 km$ , which serves as the outermost point of the disk. The innermost point from which the neutrinos can contribute in the EDR is the MPR, which is  $4 km$  from the centre. The same two points for the slowly rotating star are  $12 km$  and  $4.7 km$  respectively [18].

First we assume an isothermal disk, *i.e.* there is no temperature gradient (TG) along the disk. Figure 2 shows the variation of the EDR along the rotation axis of the star for three different temperature ( $1 MeV$ ,  $5 MeV$  and  $10 MeV$ ). Initially the EDR increases with distance and it reaches a maximum value at a distance of  $16 km$  and after that it falls off gradually. The EDR is maximum for central temperature  $T_C = 10 MeV$  and minimum for  $T_C = 1 MeV$ , which shows that the EDR increases with increase in temperature of the disk. For  $T_C = 10 MeV$  the maximum EDR is at a point about  $16 km$  and the value of EDR is  $3.3 \times 10^{47} erg/s$ , and the total energy deposited per second in the vicinity of the star (calculated by integrating EDR) is of the order of  $10^{49} erg$ . If we further increase the temperature to  $20 MeV$  the total energy deposited per second near the star is of the order of  $10^{51} - 10^{52} erg$ , close to that of the energy liberated during GRBs.

Let us try to understand the peculiar nature of initial increase in EDR with distance. From figure 3, for the isothermal disk the temperature  $T_0$ , seen by an observer at infinity, increases as the distance from the star increases. In this case  $T_0$  becomes hotter with distance and therefore it approaches  $T_{eff}$  (equal to  $T_C$  for isothermal disk) at large distance. The

EDR via neutrino pair annihilation is strongly dependent on disk temperature. Therefore let us calculate the pair annihilation of neutrinos emitted from the disk with TG. There is no definite theory governing the temperature gradient of the disk and we adopt the temperature gradient to be  $1/r$  as the simplest acceptable model adopted by others for similar calculation [11, 16]. For comparison we also plot curves with  $TG = 1/r^{1/2}$ . Due to variation of disk temperature, the temperature at the MPR (initial temperature from which our calculation starts) is much less than that of the central temperature. For  $T_C = 10MeV$  and  $TG = 1/r$  the  $T_0$  at MPR is less than  $2MeV$  and the temperature falls very rapidly and reaches fractional values beyond  $50km$ . The case of  $TG = 1/r^{1/2}$  the situation is not so pessimistic. For the hotter star,  $T_0$  at the MPR is above  $3MeV$  and does not falls to zero at large distances.

Looking at figure 4, for the isothermal disk, we see that  $F(r)$  decreases with distance and falls to zero after  $25km$ . For the disk with temperature gradient we see that  $F(r)$  initially increases and after about  $8km$  it starts to fall, unlike the previous isothermal case where it decreases throughout.

Initially for the isothermal disk the temperature dominates and EDR increases but after some distance (where  $F(r)$  decreases but temperature increases)  $F(r)$  becomes the dominating factor and the EDR decreases. The disk temperature observed at infinity is higher at outer region and the EDR increases with temperature, on the other hand the Doppler effect due to disk rotation reduces the EDR. The EDR calculated non relativistically at the MPR is half that of the relativistic case.

Figure 5 shows the variation of EDR, for disk with TG, along the rotation axis of the star for two different central temperatures  $5MeV$  and  $10MeV$ . For  $T_C = 10MeV$  with  $TG = 1/r$ , the initial value of EDR is  $10^{40}erg/s$  and it falls very sharply to zero at a distance of  $50km$ . For  $T_C = 5MeV$  the fall is even sharper. For  $TG = 1/r^{1/2}$  the fall in EDR is much slower and near the MPR the EDR, for central temperature  $T_C = 10MeV$ , is of the order of  $10^{43}erg/s$ . For the colder disk the initial EDR is much smaller. These curves show that the EDR is very sensitive to temperature as well as to TG. At low  $r$ , temperature is the governing factor in determining the nature of EDR, therefore EDR decreases. As  $r$  increase  $F(r)$ , which strongly decreases with  $r$ , becomes the dominant factor and EDR decreases further. This is why the EDR falls off much faster than the isothermal case.

The slowly rotating star has a much smaller disk (smaller equatorial plane) and its MPR



is  $4.7km$ , larger than the keplerian star. Figure 6, 7, 8, 9 depicts the various aspects of EDR for a slowly rotating star. The gross nature of the EDR for the isothermal case is more or less same, but the value of maximum EDR is slightly larger. The temperature plot is about the same, but the nature of  $F(r)$  is slightly different, the maximum value of  $F(r)$  being slightly larger. Due to this reason the EDR for the slow star is greater (twice) than that for the keplerian star. The rotational velocity seems to have some negative effect on the EDR and as the rotational velocity increases the EDR decreases.

The value of EDR increases if we go inwards from the MPR. For any star (keplerian or slow) if we go close towards the centre, the EDR increases due to the increase in temperature of the disk. Near the centre the value of EDR for non relativistic calculation and that with GR effect along with TG becomes the same. But as we go outwards the value of the EDR for the GR calculation becomes less than the non-relativistic case. This is because, for GR calculation, the disk temperature falls as we go outwards along the disk.

## V. SUMMARY AND DISCUSSION

In this article we have investigated the GR effect on the EDR of  $\nu\bar{\nu} \rightarrow e^+e^-$  reaction in a rotating neutron star described by CST metric. Here we have calculated the EDR for the neutrinos coming out of the equatorial disk and depositing energy along the rotation axis of the star, above the equatorial plane. The bending of the neutrino trajectories, and the redshift due to disk rotation along with gravitation has been taken into consideration.

We find that for an isothermal disk, initially the EDR increases with distance and reaches a maximum value and then decreases with distance. This is due to the fact that there is a competition between the temperature and the Doppler effect due to disk rotation (characterized by  $F(r)$ ). The temperature observed by the observer at infinity ( $T_0$ ) increases and at large distance becomes same as that of the effective temperature ( $T_{eff}$ ) whereas  $F(r)$  decreases with increase in distance from the disk. In the case of disk with TG, the EDR falls off very quickly with distance. For  $TG = 1/r$  the slope with which EDR falls is much greater than that for  $TG = 1/r^{1/2}$ . The  $F(r)$  increases initially but it also decreases after some distance and falls very near to zero at about  $50km$ . Both the isothermal and TG picture shows that the EDR is a very sensitive function of temperature, and as temperature decreases the EDR also decreases. The slow star shows more or less the same nature only

with the fact that EDR for the slow star is about twice that for the keplerian star. The rotational effect reduces the EDR.

To summarize, we find that the EDR is very sensitive both to the temperature and TG of the disk. The deposition energy is contributed mainly by the neutrinos arriving from the central region where the temperature is higher. The maximum energy is deposited near the surface. As we move outwards the deposition energy reduces and is smaller than that of the non relativistic calculation.

The total energy deposition from a neutron star would also depend on the off-axis contributions. So to get an estimate of the total deposition energy, one needs to do a detailed numerical simulation taking into account all possible contributions. Such a calculation is in progress and we hope to report it in the near future.

### Acknowledgments

R.M. and A.B. would like to thank CSIR, New Delhi, for financial support. A.B also thanks UGC for support. S.K.G. and S.R thank DST, Govt of India, for financial support.

- 
- [1] R. Klebsadel, I. Strong and R. Olsen, *Astrophys. J.* **182**, L85 (1973)
  - [2] A. S. Fruchter *et al.*, *Astrophys. J.* **314**, L7 (1999)
  - [3] S. Covino *et al.*, *Astronomy&Astrophysics* **348**, L1 (1999)
  - [4] A. Bhattacharyya, S. K. Ghosh, P. Joarder, R. Mallick and S. Raha, *Phys. Rev. C* **74**, 065804 (2006)
  - [5] A. Bhattacharyya, S. K. Ghosh, R. Mallick and S. Raha, *Phys. Rev. C* **76**, 052801 (2007)
  - [6] R. Mallick, S. K. Ghosh and S. Raha, *ArXiv* 0904.3393 (2009)
  - [7] S. K. Ghosh, S. C. Phatak and P. K. Sahu, *Nucl. Phys. A* **596**, 670 (1996)
  - [8] J. Alam, S. Raha and B. Sinha, *Phys. Rep.* **273**, 243 (1996)
  - [9] A. Bhattacharyya, S. K. Ghosh, S. Raha, *Phys. Lett. B* **635**, 195 (2006)
  - [10] J. Cooperstein, L. J. van der Horn and E. Baron, *Astrophys. J.* **309**, 653 (1986)
  - [11] J. Goodman, A. Dar and S. Nussinov, *Astrophys. J.* **314**, L7 (1987)
  - [12] J. D. Salmonson and J. R. Wilson, *Astrophys. J.* **517**, 859 (1999)

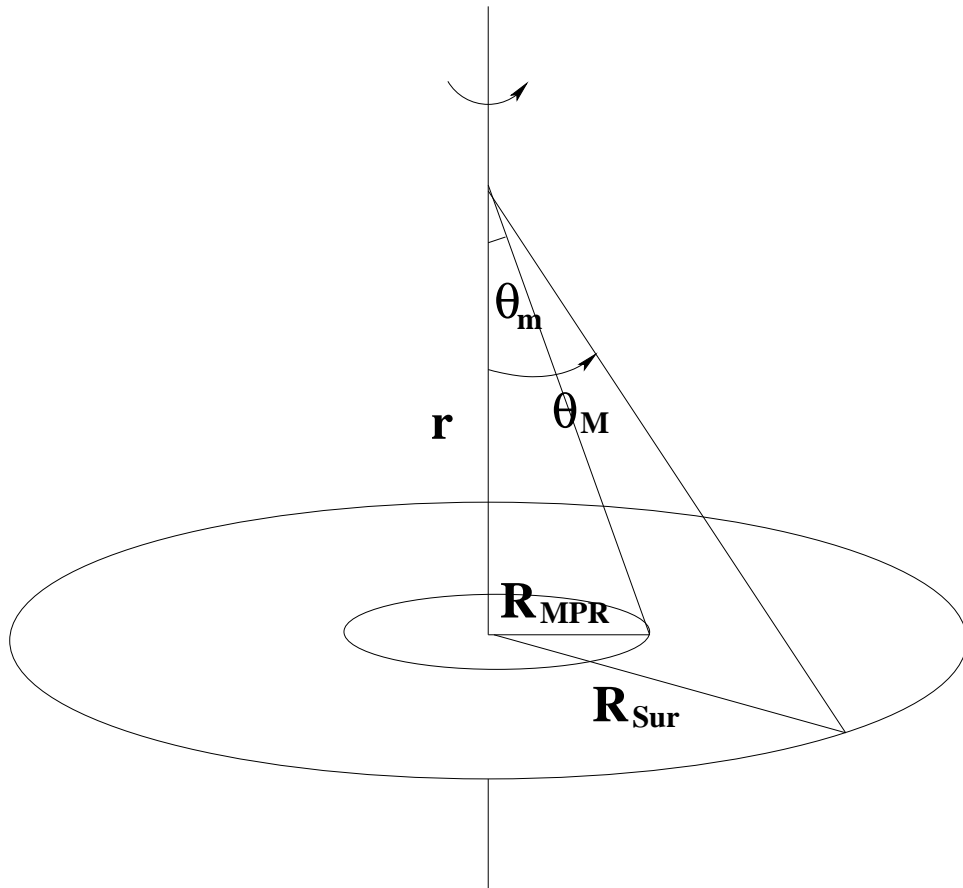


FIG. 1: Figure showing the layout of our problem. The neutrinos (antineutrinos) coming out of the equatorial plane, at an angle  $(\theta_M - \theta_m)$  and depositing their energy along the rotation axis.

- [13] J. D. Salmonson and J. R. Wilson, *Astrophys. J.* **578**, 310 (2002)
- [14] A. R. Prasanna and S. Goswami, *Phys. Lett. B* **526**, 27 (2001)
- [15] K. Asano and T. Fukuyama, *Astrophys. J.* **531**, 949 (2000)
- [16] K. Asano and T. Fukuyama, *Astrophys. J.* **546**, 1019 (2001)
- [17] R. Birkel, M. A. Aloy, H. -Th. Janka and E. Mueller, *Astronomy & Astrophysics* **463**, 51 (2007)
- [18] R. Mallick and S. Majumder, *Phys. Rev. D* **79**, 023001 (2009)
- [19] G. B. Cook, S. L. Shapiro and S. A. Teukolsky, *Astrophys. J.* **398**, 203 (1992)
- [20] H. Komatsu, Y. Eriguchi and I. Hachisu, *Mon. Not. R. Astron. Soc.* **237**, 355 (1989)
- [21] A. Bhattacharyya, S. K. Ghosh, M. Hanauske and S. Raha, *Phys. Rev. C* **71**, 048801 (2005)
- [22] N. Stergioulas and J. L. Friedman, *Astrophys. J.* **444**, 306-311 (1995)
- [23] J. Ellis, J. I. Kapusta and K. A. Olive, *Nucl. Phys. B* **348**, 345 (1991)

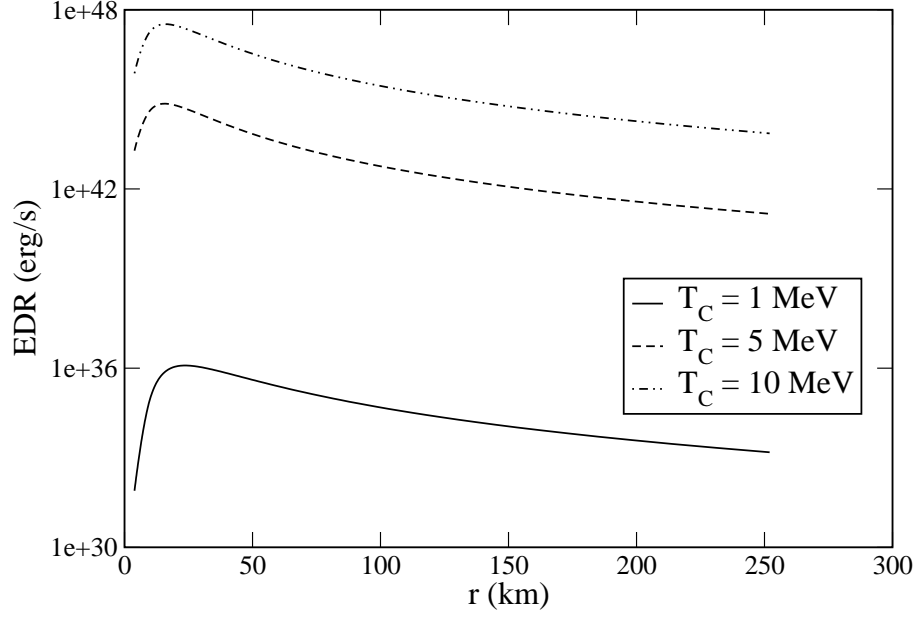


FIG. 2: Variation of EDR with distance along the rotation axis for the keplerian star having isothermal disk with three different central temperature.

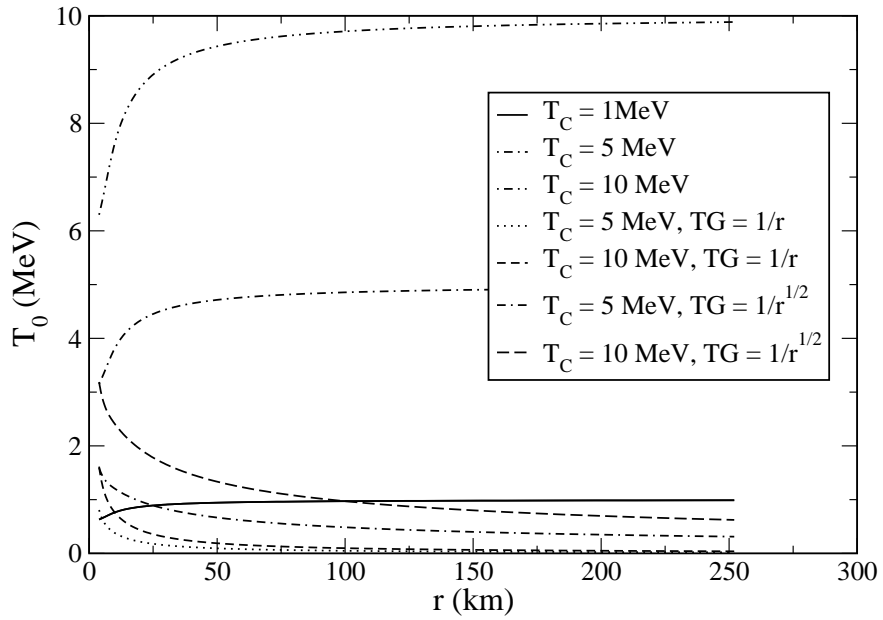


FIG. 3: Variation of temperature  $T_0$  with distance along the rotation axis of the keplerian star.  $T_0$  is plotted for both isothermal disk and for disk having two different temperature gradient.

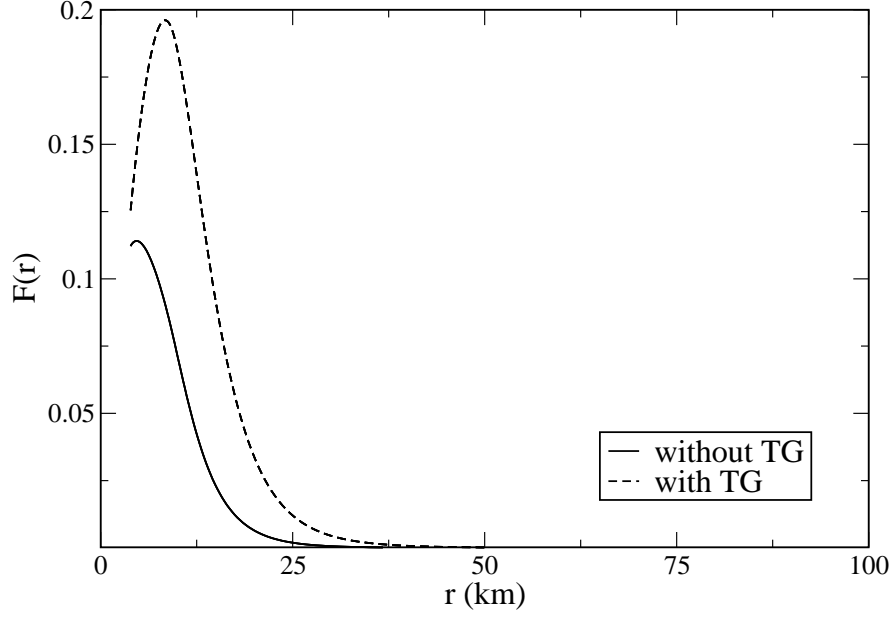


FIG. 4: Variation of  $F(r)$  with distance along the rotation axis of the keplerian star.  $F(r)$  is plotted both for isothermal disk and disk with temperature gradient.

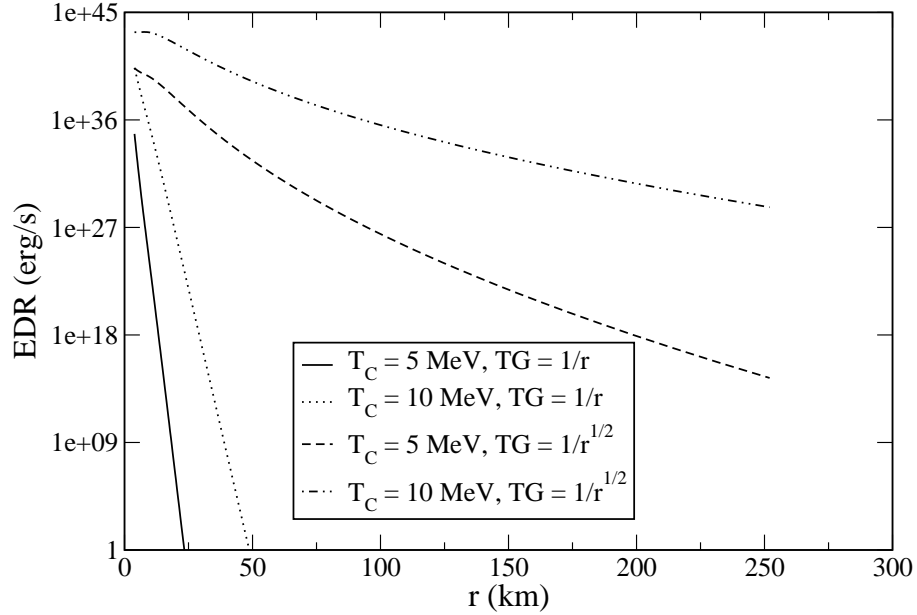


FIG. 5: Variation of EDR with distance along the rotation axis for the keplerian star. The plot have been done with disk having two different TG and the curves are plotted with two different central temperature.

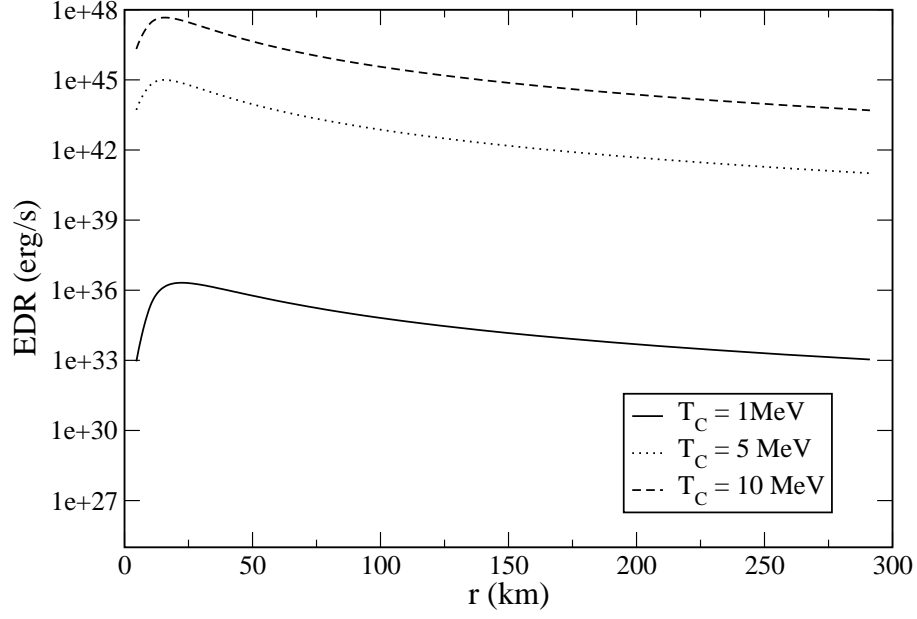


FIG. 6: Variation of EDR with distance along the rotation axis for the slow star having isothermal disk with three different central temperature.

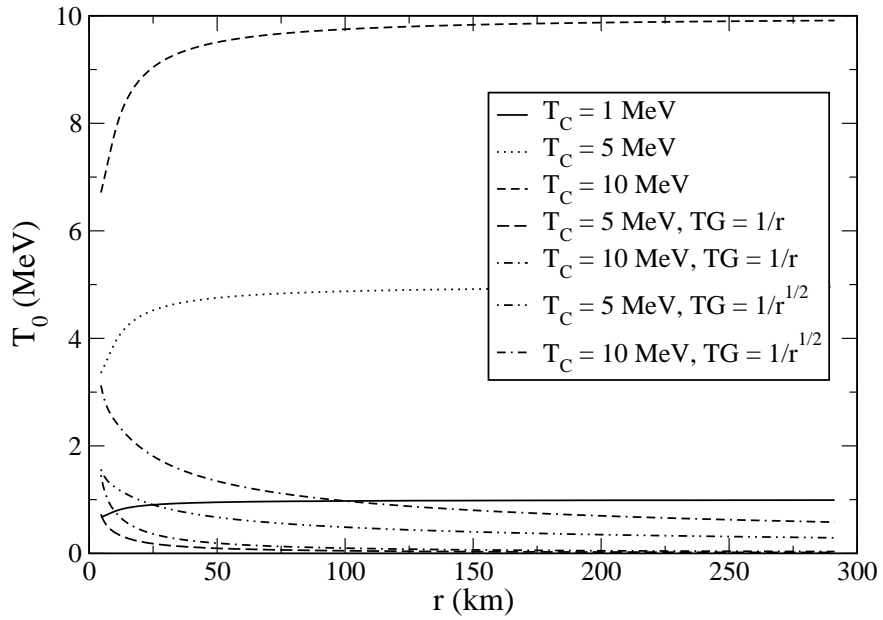


FIG. 7: Variation of temperature  $T_0$  with distance along the rotation axis of the slow star.  $T_0$  is plotted for both isothermal disk and for disk having two different temperature gradient.

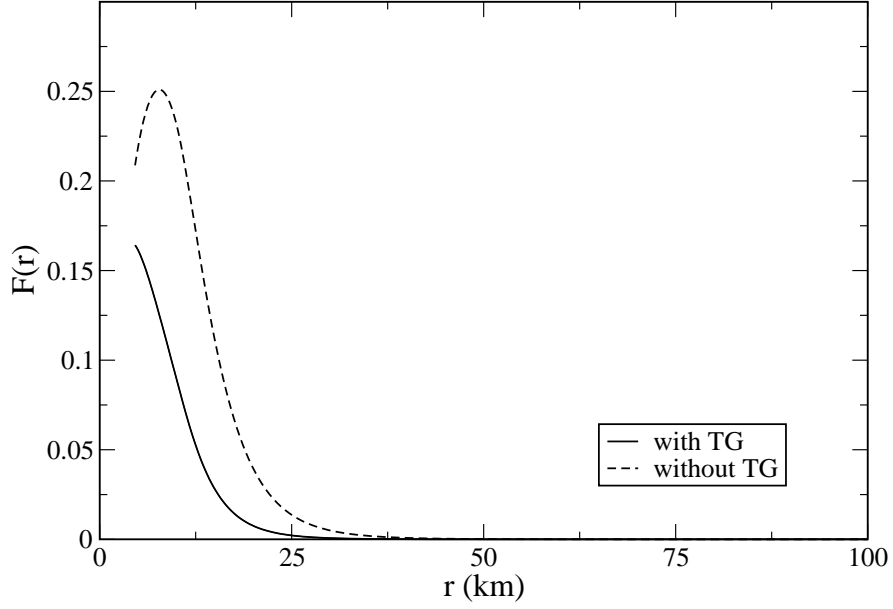


FIG. 8: Variation of  $F(r)$  with distance along the rotation axis of the slow star.  $F(r)$  is plotted both for isothermal disk and disk with temperature gradient.

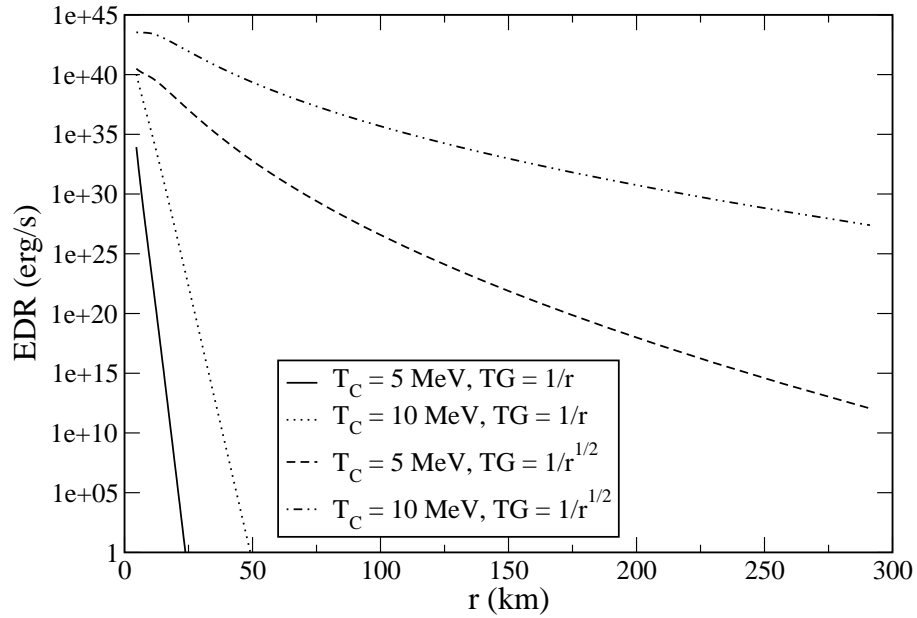


FIG. 9: Variation of EDR with distance along the rotation axis for the slow star. The plot have been done with the disk having two different TG and the curves are plotted with two different central temperature.